Lithium Isotope Effect Accompanying Electrochemical Intercalation of Lithium into Graphite

Satoshi Yanase, Wakana Hayama, and Takao Oi

Department of Chemistry, Sophia University, 7-1 Kioicho, Chiyoda, Tokyo 102-8554, Japan

Reprint requests to Prof. T. Oi: Fax: 81-3-3238-3361; E-mail: t-ooi@sophia.ac.jp

Z. Naturforsch. **58a,** 306 – 312 (2003); received January 3, 2003

Lithium has been electrochemically intercalated from a 1:2 (v/v) mixed solution of ethylene carbonate (EC) and methylethyl carbonate (MEC) containing 1 M $LiClO_4$ into graphite, and the lithium isotope fractionation accompanying the intercalation was observed. The lighter isotope was preferentially fractionated into graphite. The single-stage lithium isotope separation factor ranged from 1.007 to 1.025 at 25 °C and depended little on the mole ratio of lithium to carbon of the lithium-graphite intercalation compounds (Li-GIC) formed. The separation factor inceased with the relative content of lithium. This dependence seems consistent with the existence of an equilibrium isotope effect between the solvated lithium ion in the EC/MEC electrolyte solution and the lithium in graphite, and with the formation of a solid electrolyte interfaces on graphite at the early stage of intercalation.

Key words: Lithium Isotopes; Isotope Effects; Electrochemical Intercalation, Single-stage Separation Factor; Lithium-graphite Intercalation Compounds.

1. Introduction

Graphite forms various graphite intercalation compounds (GICs), which are layered compounds, by taking up materials such as alkali metals, halogens and metal halides between its graphene layers [1, 2]. A characteristic property of GICs is the staging phenomenon, the staged structure being given in terms of the stage index that denotes the number of graphene layers between adjacent intercalate layers [3]. Lithium can be intercalated chemically and electrochemically into graphite to form Li-GICs. Four different staged structures of Li-GICs are known, the maximum amount of intercalated lithium corresponding to LiC_6.

Charge-discharge reactions of lithium ion secondary batteries are used as energy sources of various portable electronic devices [3, 4]. A typical lithium ion secondary battery is composed of an anode made of a lithium oxide-based compound such as $LiCoO_2$, a graphite cathode and an organic electrolyte containing a lithium salt. It is charged and discharged by intercalating and deintercalating lithium ions, and a battery voltage of 3 to 4 V is achieved. The chemical reaction occurring is in principle the redox reaction of lithium between Li^0 and Li^+. Tin compounds are studied as substitutes of graphite due to their large capacity for lithium [5].

On the other hand, the isotopes of lithium have important applications in nuclear science and industry. The largest demand for the isolated or enriched lighter isotope, ^{6}Li, will be in DT fusion power reactors where lithium compounds rich in ^{6}Li will be required for the tritium breeder blanket: ^{6}Li + n $\rightarrow$ T + ^{4}He. Various methods of lithium isotope separation have been developed. They include amalgam [6 – 8], ion exchange [9,10], crown ether-cryptand [11] and electromigration [12] methods. Among them, the only method that was applied for a large-scale lithium isotope separation is the amalgam method. In this method, lithium is distributed between the amalgam phase and an aqueous or organic electrolyte phase, the lithium isotope separation is being based on the equation

$$^7\mathrm{Li(Hg)} + {}^6\mathrm{Li(SOL)}^+ = {}^6\mathrm{Li(Hg)} + {}^7\mathrm{Li(SOL)}^+. \quad (1)$$

The oxidation state of lithium is formally 0 in the amalgam and +1 in the solution. Thus the lithium isotope effects of (1) are based on the redox reaction of lithium. The reported value of the equilibrium constant of (1) is $1.049 \sim 1.062$ [7], larger than those reported for ion exchange and crown-ether systems, where no change of the oxidation state of lithium occurs.

Although the large lithium isotope effect accompanying the redox reaction of lithium is attractive, the use of toxic mercury makes the amalgam method difficult

to be applied to large-scale lithium isotope enrichment in the future. Thus, it seems important to seek material that is not toxic and can still be used for lithium isotope separation utilizing the redox reaction. In this context we paid attention to graphite. As mentioned above, the reaction occurring at the graphite electrode of a lithium ion secondary battery is basically the redox reaction of lithium. Consequently, if the lithium isotope effect accompanying such a reaction is large, charge-discharge of lithium ion secondary batteries may be applied to the lithium isotope separation in a practical sense.

We carried out experiments in which lithium was electrochemically intercalated into graphite from an organic lithium ion-bearing electrolyte solution and observed lithium isotope effects accompanying the intercalation. This paper reports the results of such experiments.

2. Experimental

2.1. Graphite and Reagents

Graphite flakes with grain sizes of less than 180 μm were used as host material. Lithium foils, 1 mm thick and with a purity of 99.8%, were purchased from Honjo Metals Co. Ltd. A 1:2 v/v mixed solution of ethylene carbonate (EC) and methylethyl carbonate (MEC) containing 1 M $LiClO_4$, (LIPASTE-E2MEC/1), used as organic electrolyte solution, was purchased from Tomiyama Pure Chemical Industries Ltd. An N-methylpyrrolidone (82 wt%) solution of polyvinylidene fluoride (18 wt%) (Kureha Chemical Industry Co., Ltd., KF polymer-L #1120) was used as a gluing agent. 50 μm copper foils, manufactured by Furukawa Electric Co., Ltd., were used as basal plates of the graphite electrodes. The other reagents were of analytical grade and were used without further purification except hexane, which was used after dehydration with molecular sieves.

2.2. Electrochemical Intercalation of Lithium into Graphite

The experimental apparatus used, schematically drawn in Fig. 1, is basically the same as the one used in the experiments in which lithium was electrochemically inserted into tin metal [13]. It was composed of a power supply (a Hokuto Denko Corporation HJ-201B battery charge / discharge unit), a three-electrode electrochemical cell (electrolytic cell) and a data acquisition unit consisting of an A/D converter and a personal computer. Lithium foils of about 7 mm × 7 mm size, attached to stainless steel meshes by pressing, were used as anode and reference electrode. The graphite cathode was made as follows: Graphite flakes and the N-methylpyrrolidone solution with weight ratios of 4:1 to 2:1 were first mixed to obtain a homogeneous graphite paste. This paste was daubed manually on a copper foil as uniformly as possible. The copper foil with the paste on it was heated at 120 ℃ for 20 min to remove the N-methylpyrrolidone component of the paste and finally to obtain a cathode of graphite laminated on a copper foil. A SEM photo of the surface of a graphite cathode is shown in Figure 2. The size of the laminated graphite cathode was about 1.6 cm × 1.6 cm × 100 μm. The electrolytic cell was build up in a dry argon atmosphere. The volume of the electrolyte solution was about 30 cm^3 and the cathode was placed so that the laminated graphite was wholly immersed in the electrolyte.

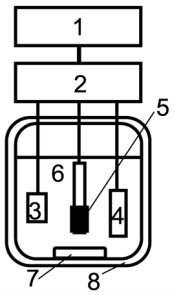

Fig. 1. The experimental apparatus. 1, data acquisition unit; 2, power supply; 3, lithium reference electrode; 4, lithium anode; 5, graphite cathode; 6, electrolyte solution; 7, stirrer tip; 8, electrolytic cell.

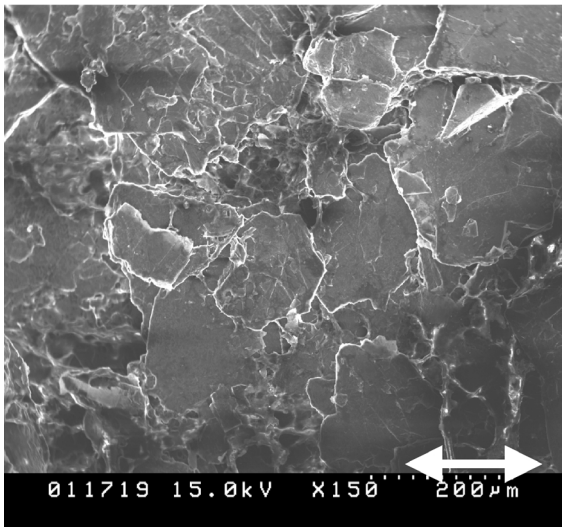

Fig. 2. A SEM photo of the surface of a graphite electrode.

The lithium intercalation was performed in the constant current-constant voltage mode. That is, the electrolysis (lithium intercalation) was at first carried out in a constant current mode (3 mA). As the electrolysis proceeded, the electric potential of the cathode against the lithium reference electrode (cathode potential), which was at first around 3.1 V, quite swiftly decreased and reached the pre-determined value set at 0.02 to 0.15 V. The electrolytic mode was then automatically changed to the constant voltage mode; the electrolysis was continued and the electric current gradually decreased while keeping the cathode potential constant at the predetermined value. The electrolysis continued until the integrated quantity of electricity reached the predetermined value of 6 to 55 C and was discontinued manually. During the electrolysis, the temperature of the electrolytic cell was kept at 25 ℃ and the electrolyte solution was stirred by a magnetic stirrer.

2.3. Analyses

After the electrolysis was finished, the graphite cathode was taken out of the cell in a dry argon atmosphere, washed thoroughly with dehydrated hexane and was allowed to stand for a day to remove adhering hexane by evaporation. The Li-GIC formed on the copper foil of the cathode was stoichiometrically recovered from the foil and heated in an aluminum crucible placed in an electric furnace at 800 ℃ for 10 hours to convert the chemical form of the intercalated lithium into lithium oxide. This lithium oxide was dissolved with 2 M HCl to obtain a lithium chloride solution. Part of the solution was used for the determination of the amount of the intercalated lithium by measuring the lithium concentration of the solution with a Dainiseikosha SAS727 atomic absorption spectrometer operated in the flame photometric mode. The remainder of the solution was used for the lithium isotope analysis. Details of $^{7}Li/^{6}Li$ isotopic ratio measurements were described in [9]. A part of the electrolyte solution after the electrolysis was also heated in the electric furnace at 800 ℃ for 10 hours, and the resultant lithium oxide underwent the same treatment as the lithium oxide from the Li-GIC to determine the lithium isotopic ratio. The separation factor, S, defined as $S = (^{7}Li/^{6}Li)_{electrolyte}/(^{7}Li/^{6}Li)_{graphite}$ was then calculated. By definition, S is larger than unity when the lighter isotope is preferentially fractionated into the graphite phase.

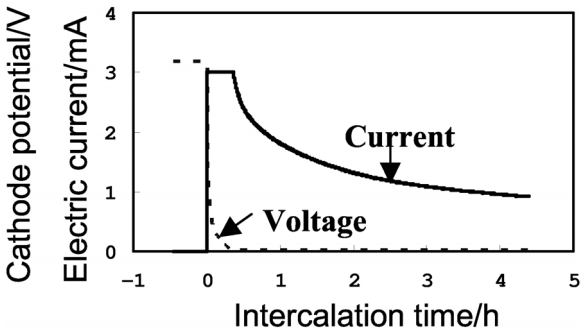

Fig. 3. An example of the cathode potential and the electric current changes as functions of the intercalation time.

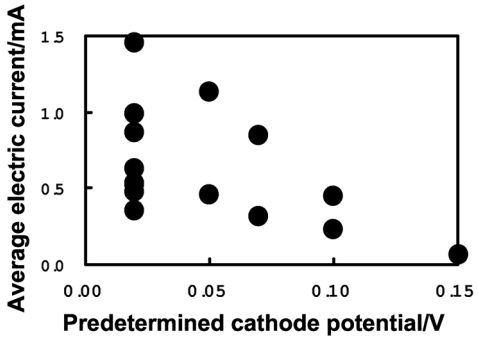

Fig. 4. Plot of the average electric current against the predetermined cathode potential.

3. Results and Discussion

Experimental conditions and results are summarized in Table 1. The amount of graphite flakes used for the graphite cathodes ranged from 1.43 to 4.41 mmol. The integrated quantity of electricity was varied from 6.1 to 54.5 C, and the chemical formula of the formed Li-GICs calculated from the integrated quantities of electricity and the amount of graphite flakes loaded on the copper foils was from $Li_{0.029}C$ to $Li_{0.16}C$. An example of the changes of the cathode potential and the electric current during an electrolytic course (Run LC2-3) is shown in Figure 3. The cathode potential swiftly decreased at the very beginning of the electrolysis, reached the predetermined value (0.02 V in this case) and was kept constant thereafter. The electric current was kept constant (3 mA) until the cathode potential reached the predetermined value, and then it started decreasing. The rate of the decrease in electric current was large at first and gradually became small. The intercalation time ranged from 3.75 to 35 hours.

Table 1. Experimental conditions and results.

Run No.	Predetermined cathode potential/V	Amount of carbon in graphite cathode/mmol	Integrated quantity of electricity/C	Intercalation time/h	Average electric current/mA	*m* in Li_mC[a] A	*m* in Li_mC[b] B	Current efficiency[c] / %	*S*
LC2-1	0.02	1.83	12.7	6.58	0.534	0.072	0.061	84	1.014
LC2-2	0.02	2.96	19.4	10.35	0.520	0.068	0.041	60	1.020
LC2-3	0.02	3.41	23.0	4.38	1.456	0.070	0.049	71	1.009
LC2-4	0.02	2.79	26.2	11.70	0.622	0.097	0.106	109	1.009
LC2-5	0.02	2.73	26.4	8.47	0.866	0.100	0.102	102	1.018
LC2-6	0.02	3.85	29.0	8.18	0.986	0.078	0.075	96	1.017
LC2-7	0.02	3.58	34.8	11.17	0.865	0.101	0.085	84	1.015
LC2-8	0.02	2.89	43.7	35.00	0.347	0.157	0.126	80	1.020
LC2-9	0.02	3.59	54.5	32.20	0.470	0.157	0.137	87	1.025
LC5-1	0.05	1.79	12.4	7.58	0.454	0.072	0.053	73	1.020
LC5-2	0.05	4.41	30.1	7.42	1.126	0.071	0.062	87	1.010
LC7-1	0.07	1.74	11.8	10.40	0.314	0.070	0.079	112	1.015
LC7-2	0.07	3.25	20.2	6.67	0.843	0.065	0.051	79	1.012
LC10-1	0.10	1.56	6.08	3.75	0.450	0.040	0.048	120	1.007
LC10-2	0.10	1.43	6.27	7.50	0.232	0.045	0.051	112	1.010
LC15	0.15	2.25	6.48	29.25	0.061	0.030	0.032	108	1.009

[a] Calculated from the integrated quantity of electricity. [b] Determined by the chemical analysis of Li-GIC. [c] 100 × B/A.

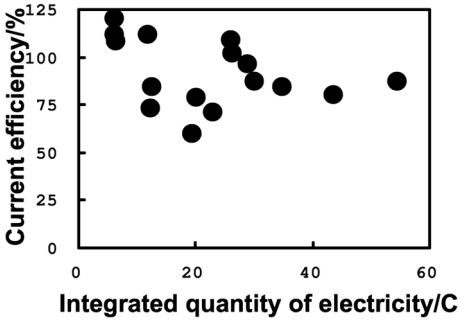

Fig. 5. Plot of the current efficiency against the integrated quantity of electricity.

It was observed that, as the electrolysis proceeded, the color of graphite changed from black to gold, showing the formation of the stage-1 Li-GIC [2]. The chemical reaction occurring may be expressed as

$$C + mLi^+ + me^- \rightarrow Li_mC, \quad (2)$$

and the maximum achievable value of *m* is 0.17. In many runs, the gold color disappeared after the electrolysis, most probably due to the diffusion of intercalated lithium atoms within graphite and/or to edge surfaces.

In Fig. 4, the mean electric current is plotted against the predetermined cathode potential. As expected from the fact that the low predetermined cathode potential corresponds to a large potential drop during the electrolysis, the mean electric current is in general higher for the lower predetermined cathode potential. That is, the low predetermined cathode potential corresponded to the high electric current (the high electric current density) and consequently to the fast reaction rate of (2).

In Fig. 5, the current efficiency (%), 100 times the ratio of the amount of intercalated lithium determined by the chemical analysis of the Li-GIC formed to that from the integrated quantity of electricity and the amount of graphite flakes used for the cathode, is plotted against the integrated quantity of electricity. It seems independent of the integrated quantity of electricity, although the data are scattered substantially, ranging from 60 to 120%. The reason for a current efficiency of more than 100% is not very clear; it must be due in part to experimental errors and/or may be due to insufficient washing of the cathode with hexane. The current efficiency below 100% indicates, in addition to experimental errors, the existence of some side reactions other than (2), such as the reduction of EC molecules of the electrolyte solution [14]: $2Li^+ + 2EC + 2e^- \rightarrow LiOCO_2CH_2CH_2OCO_2Li + C_2H_4$. In fact, evolution of gas on the cathode surface was recognized during the electrolysis, especially at the early stage of the electrolysis where both the cathode potential and the electric current were high. If the reaction product, $LiOCO_2CH_2CH_2OCO_2Li$, remained in the electrolyte without adhering to the graphite electrode surface, it would lead to a decrease in current efficiency.

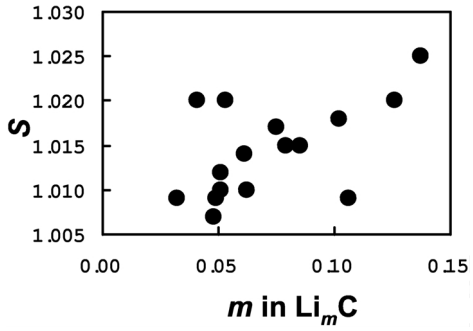

Fig. 6. Plot of S against m in Li_mC.

3.1. Lithium Isotope Effects

The separation factor data are listed in the last column of Table 1. All the S values are larger than unity, ranging from 1.007 to 1.025, which shows that the lighter isotope was preferentially intercalated into graphite in every experiment. However, the maximum S value of 1.025 is much smaller than those of the amalgam method [7].

The S value is plotted against m in Li_mC determined by the chemical analysis in Figure 6. A shallow correlation is observed between S and m, indicating that the Li-GIC with the larger Li content shows the larger lithium isotope effect, although the degree of data scattering is substantial.

Intercalation of lithium into graphite may be divided into four processes; (i) diffusion of solvated lithium ions in the electrolyte solution to edge surfaces of graphite, (ii) desolvation of solvated lithium ions at edge surfaces, (iii) intercalation of lithium ions between graphene layers (reduction of lithium ions to neutral lithium atoms), and (iv) diffusion of intercalated lithium atoms within graphite. The isotopic composition of the intercalated lithium cannot be changed by diffusion within graphite. Process (iv) does thus not contribute to the lithium isotope effects observed in the present work. Process (i) is the process in which solvated lithium ions diffuse in the bulk electrolyte solution and the lighter isotope may faster. Okamoto and Kakihana [15] reported that an S value of 1.008 was observed in the electromigration of lithium ions in a cation exchange membrane and could be explained by the migration of the hydrated lithium ions, $Li^+(H_2O)_n$ with n being around 3. That is, S is given by the square root of the ratio of the mass of the hydrated heavier isotopic ion to that of the hydrated lighter isotopic ion. This type of isotope effect may exist in process (i). Lithium ions are selectively coordinated by EC molecules in the EC/MEC mixed solution and the solvation number of the lithium ion is four in the primary solvation sphere [16,17]. The separation factor, S_{dif}, expected for the diffusion process of $Li^+(EC)_4$ in the electrolyte is then estimated to be 1.0014, much smaller than the S values observed in this work. It must become even smaller if secondary and higher-order solvation spheres are also taken into consideration. Thus, diffusion of the solvated lithium ion in the electrolyte solution towards edge surfaces of graphite is expected to contribute only slightly, if at all, to the observed lithium isotope effects.

The equilibrium lithium isotope effects in processes (ii) and (iii) may be expressed as

$$^6Li^+(SOL) + {}^7Li^+(SURFACE) = {}^7Li^+(SOL) + {}^6Li^+(SURFACE), \quad (3\text{-}1)$$

and

$$^6Li^+(SURFACE) + {}^7Li_mC = {}^7Li^+(SURFACE) + {}^6Li_mC, \quad (3\text{-}2)$$

respectively. In (3-1) and (3-2), $Li^+(SOL)$ denotes the solvated lithium, $Li^+(SURFACE)$ the desolvated lithium ion at edge surfaces and Li_mC the lithium atom in the Li-GIC. As mentioned above, $Li^+(SOL)$ is most probably $Li^+(EC)_4$ if selective solvation of EC occurs and only the solvation in the primary solvation sphere is considered. The isotope effect in (3-1) is the one accompanying solvation of the lithium ion (or desolvation of the solvated lithium ion), and that in (3-2) the one accompanying the reduction of the lithium ion to neutral lithium and the bond formation between a lithium atom and carbon atoms within graphite. The combination of (3-1) and (3-2) gives

$$^6Li^+(SOL) + {}^7Li_mC = {}^7Li^+(SOL) + {}^6Li_mC. \quad (3\text{-}3)$$

Equation (3-3) represents the lithium isotope exchange reaction between the EC/MEC mixed electrolyte solution phase and the graphite phase. Assuming that the obtained separation factors are based on equilibrium isotope effects, the experimental results show that the equilibrium constant, K, of (3- 3) is larger than unity, although the equilibrium constants of its constituent reactions (3-1) and (3-2) cannot be individually known.

Based on the theory of isotope effects by Bigeleisen and Mayer [18], K of (3-3) is the ratio of the reduced partition function ratios (RPFRs), $(s/s')f$, of the chemical species, $Li^+(SOL)$ and Li_mC, as,

$$K = (s/s')f_{\text{electrolyte}}/s/s')f_{\text{graphite}}, \quad (4)$$

where $(s/s')f_{\text{electrolyte}}$ and $(s/s')f_{\text{graphite}}$ are the RPFRs of lithium in the electrolyte phase (*i. e.*, Li^+(SOL)) and in the graphite phase (*i. e.*, Li_mC), respectively. The experimental results are consistent with the relation $(s/s')f_{\text{electrolyte}} > (s/s')f_{\text{graphite}}$. The RPFRs are calculable if information on the molecular vibrations is available. Unfortunately, no lithium-related frequency is reported for the lithium ion in the EC/MEC electrolyte solution or the lithium atom in Li-GICs. We [19] demonstrated that the vibrational analysis based on the molecular orbital (MO) theory was effective for such systems where no experimental molecular vibrational frequency is available. MO calculations on lithium species modeling those in the EC/MEC electrolyte and Li-GICs are in progress, and part of calculations has already been published [17].

In a previous paper on chemical insertion of lithium into graphite [20], it was observed that *S* is independent of *m* in Li_mC between 0.065 and 0.17. The present results show that *S* is shallowly dependent on *m* in the range *m* = 0.032 to 0.14. If the observed *S* is solely based on the equilibrium isotope effect of (3-3), it should be independent of *m*. The present results thus indicated that some other effect is involved. The most plausible effect is the formation of surface films on the graphite electrodes. It is generally accepted that stable surface films are formed on graphite electrodes in the EC-based solutions upon the first charging, and thereby the carbon surface is passivated [3]. The film, often called "solid electrolyte interface (SEI)" [21], has lithium-ion conductivity but does not show electronic conductivity. The film, once formed, suppresses further solvent decomposition, but through this film lithium ions can be intercalated within graphite. According to Ogumi and Inaba [3], solvated lithium ions are intercalated between graphene layers, and this stable passivating layer (*i. e.*, SEI) is formed by accumulation of decomposition products of the solvated lithium ions and by rupturing of the graphene layers. This kind of film may also be formed at the early stage of each experiment in this work. The RPFR of this film is expected to be close to that of the solvated lithium ion in the EC/MEC electrolyte solution because lithium in the film is derived from the lithium ion in the electrolyte without accompaniment of equilibrium isotope effects and, as mentioned before, the kinetic isotope effect upon transportation of solvated lithium ions in the electrolyte to the edge surfaces of graphite is, if any, small.

The dependence of *S* on *m* in Li_mC is consistent with the formation of SEIs at the early stage of the electrolysis and the equilibrium isotope effect (3-3). At the early stage of the electrolysis in each experiment, the solvated lithium ions are intercalated in graphite, leading to the formation of SEIs. The amount of the lithium ion taken up by graphite and used for the formation of SEIs at that time may differ from experiment to experiment. The chemical analysis recognizes the lithium ions in SEIs as belonging to the graphite phase, but from the viewpoint of isotope effects, they contribute little to the separation factor. Once the film is formed, solvated lithium ions are desolvated and taken up by graphite through this film. In this process, the equilibrium isotope effect (3-3) is expected. With increasing *m*, the amount of lithium taken up after desolvation increases, which leads to the increase of *S*.

The formation of SEI may also explain the relatively large degree of *S* data scattering; If the amount of lithium ions participating in the formation of SEI differs substantially from experiment to experiment, probably mostly depending on the conditions of graphite electrodes, it necessarily contributes to *S* by different degrees. In the present work, graphite flakes with grain sizes up to 180 μm are used. With such graphite, it is difficult to produce equivalent electrodes at the microscopic level. Graphite powders with much small grain sizes may reduce scattering of *S* values.

Kinetic lithium isotope effects may also occur in the processes (ii) and (iii). However, they do not seem to be able to explain the dependence of *S* on *m* in Li_mC in Fig. 6; the *m* dependence of *S* can be explained qualitatively by the equilibrium isotope effect of (3-3) and the formation of SEIs without resorting to kinetic isotope effects.

4. Conclusion

Lithium isotope effects accompanying electrochemical intercalation of lithium from EC/MEC mixed solutions containing lithium perchlorate into graphite were experimentally observed at 25 °C. The lighter isotope was preferentially taken up by graphite in all experiments. The value of the single-stage separation factor ranged from 1.007 to 1.025 and was slightly dependent on *m* in Li_mC. This dependence seems consistent with the existence of an equilibrium isotope effect between the solvated lithium ion in the electrolyte solu-

tion and the lithium in graphite and with the formation of a solid electrolyte interface at the early stage of the electrolysis.

Acknowledgements

We thank Dr. T. Abe, Institute of Atomic Energy, Kyoto University, for donating graphite flakes, and Kureha Chemical Industry Co., Ltd. for donating a gluing agent. The use of a mass spectrometer to determine $^{7}Li/^{6}Li$ isotopic ratios was kindly offered by Prof. Y. Fujii, Res. Lab. Nucl. Reactors, Tokyo Institute of Technology. The assistance of Dr. M. Nomura, RLNR-TIT, in the $^{7}Li/^{6}Li$ isotopic ratio measurements is greatly appreciated.

[1] M. Inagaki and Y. Hishiyama, New Carbon Zairyo, Gihoudou Shuppan, p. 103 (1994) (in Japanese), and references therein.
[2] Tanso Zairyo Gakkai (ed), Shin Tanso Zairyo Nyumon, Realize inc., p. 157 (1996) (in Japanese), and references cited therein.
[3] Z. Ogumi and M. Inaba, Bull. Chem. Soc. Japan **71**, 521 (1998), and references cited therein.
[4] J. R. Dahn, T. Zheng, Y. Liu, and J. S. Xue, Science. **270**, 590 (1995), and references therein; J. R. Dahn, Phys. Rev. **B44**, 9170 (1991), and references therein; R. Fong, U. Sacken, and J. R. Dahn, J. Electrochem. Soc. **137**, 2009 (1990), and references therein.
[5] I. A. Courtney and J. R. Dahn, J. Electrochem. Soc. **144,** 2943 (1997); H. Ikuta, M. Nagayama, and M. Wakihara, Battery Technol. **10**, 25 (1998) (in Japanese); Y. Idota, T. Kubota, A. Matsufuji, Y. Maekawa, and T. Miyasaka, Science **276**, 1395 (1998); J. Yang, Y. Takeda, N. Imanishi, and O. Yamamoto, Battery Technol. **11**, 103 (1999); S. Panero, G. Savo, and B. Scrosati, Electrochem. Solid-State. Lett. **2**, 365 (1999); G. R. Goward, F. Leroux, W. P. Power, G. Ouvrard, W. Dmowski, T. Egami, and L. F. Nazar, Electrochem. Solid-State Lett. **2**, 367 (1999).
[6] A. A. Palko, J. S. Drury, and G. M. Begun, J. Chem. Phys. **64**, 1828 (1976).
[7] M. Fujie, Y. Fujii, M. Nomura, and M. Okamoto, J. Nucl. Sci. Technol. **23**, 330 (1986).
[8] B. Collen, Acta Chem. Scand. **17**, 2410 (1963); J. C. Hall, R. C. Murray. Jr, and P. A. Rock, J. Chem. Phys. **51**, 1145 (1969); G. Singh, J. C. Hall, and P. A. Rock, J. Chem. Phys. **56**, 1855 (1972); G. Singh and P. A. Rock, J. Chem. Phys. **57**, 5556 (1972); K. Okuyama, I. Okada, and N. Saito, J. Inorg. Nucl. Chem. **35**, 2883 (1973).
[9] T. Oi, K. Kawada, M. Hosoe, and H. Kakihana, Sep. Sci. Technol. **26**, 1353 (1991).
[10] T. I. Taylor and H. C. Urey, J. Chem. Phys. **5**, 597 (1937); D. A. Lee and G. M. Begun, J. Amer. Chem. Soc. **81**, 2332 (1959); D. A. Lee, J. Phys. Chem.. **64**, 187 (1960); D. A. Lee, J. Amer. Chem. Soc. **83**, 1801(1961); D. A. Lee, J. Chem. Eng. Data. **6**, 565 (1961); D. A. Lee and J. S. Drury, J. Inorg. Nucl. Chem. **27**, 1405 (1965); Z. Hagiwara and Y. Takakura, J. Nucl. Sci. Technol. **6**, 153 (1969); Z. Hagiwara and Y. Takakura, J. Nucl. Sci. Technol. **6**, 279 (1969); Z. Hagiwara and Y. Takakura, J. Nucl. Sci. Technol. **6**, 326 (1969); K. Ooi, Q. Feng, H. Kanoh, and T. Oi, Sep. Sci. Technol. **30**, 3761 (1995); T. Oi, K. Shimizu, S. Tayama, Y. Matsuno, and M. Hosoe, Sep. Sci. Technol. **34**, 805 (1999); T. Oi, Y. Uchiyama, M. Hosoe, and K. Itoh, J. Nucl. Sci. Technol. **36**, 1064 (1999); T. Oi, M. Endoh, M. Narimoto, and M. Hosoe, J. Mater. Sci. **35**, 509 (2000); H. Takahashi and T. Oi, J. Mater. Sci. **36**, 1621 (2001).
[11] K. Nishizawa, S. Ishino, H. Watanabe, and M. Shinagawa, J. Nucl. Sci. Technol. **21**, 694 (1984); K. Nishizawa, T. Takano, I. Ikeda, and M. Okahara, Sep. Sci. Technol. **23**, 333 (1988); K. Nishizawa and T. Takano, Sep. Sci. Technol. **23**, 751 (1988); S. Fujine, K. Saito, and K. Shiba, J. Nucl. Sci. Technol. **20**, 439 (1983).
[12] Y. Fujii, H. Kakihana, M. Okamoto, T. Oi, and Y. Sakuma, Isotopenpraxis **15**, 203 (1979); Y. Fujii, M. Hosoe, and M. Okamoto, Z. Naturforsch. **42**, 709 (1987); I. Okada, K. Okuyama, T. Miyamoto, I. Tomita, and N. Saito, J. Inorg. Nucl. Chem. **35**, 2957 (1973); I. Okada and N. Saito, J. Nucl. Sci. Technol. **11**, 314 (1974); I. Okada, K. Gundo, M. Nomura, Y. Fujii, and M. Okamoto, Z. Naturforsch. **41a**, 1045 (1986); T. Haibara, O. Odawara, and I. Okada, J. Electrochem. Soc. **136**, 1059 (1989).
[13] S. Yanase, T. Oi, and S. Hashikawa, J. Nucl. Sci. Technol. **37**, 919 (2000).
[14] Y. E. Eli, Solid-State Lett. **2**, 212 (1999).
[15] M. Okamoto and H. Kakihana, Nippon Kagaku Zasshii, **84**, 404(1963) (in Japanese); M. Okamoto and H. Kakihana, Nippon Kagaku Zasshii, **88**, 313(1967) (in Japanese).
[16] R. J. Blint, J. Electrochem. Soc., **142**, 696 (1995).
[17] S. Yanase and T. Oi, J. Nucl. Sci. Technol. **39**, 1060 (2002).
[18] J. Bigeleisen and M. G. Mayer, J. Chem. Phys. **15**, 261 (1947).
[19] S. Yanase and T. Oi, Z. Naturforsch. **56a**, 297 (2001); S. Yanase and T. Oi, Nukleonika, **47**, S75 (2002).
[20] S. Hashikawa, S. Yanase, and T. Oi, Z. Naturforsch. **57a**, 857 (2002).
[21] E. Peled, J. Electrochem. Soc. **126**, 2047 (1979).